



## DEVELOPMENT OF BIODEGRADABLE POROUS STARCH FOAM FOR IMPROVING ORAL DELIVERY OF EPROSARTAN MESYLATE

Sachin N. Kothawade\*, Pravin D. Chaudhari

Department of Pharmaceutics, Progressive Education Society's, Modern college of Pharmacy,  
Nigdi, Pune, Maharashtra, India

\*Corresponding author: [sachin.kothawade23@gmail.com](mailto:sachin.kothawade23@gmail.com)

### ABSTRACT

Compared to inorganic carriers, Biodegradable Porous Starch Foam has shown strong properties and has a nano-porous structure, low density and large specific surface area and pore volume of Biodegradable Porous Starch Foam to improve the solubility and enhance absorption of poorly water-soluble drugs. The study aimed to prepare Biodegradable Porous Starch Foam used to improve bioavailability of poorly water-soluble drug Eprosartan Mesylate. The solid-state properties of the loaded BPSF samples have been characterised by SEM, FTIR, XRPD, and DSC for the analysis of the state of dispersion of loaded eprosartan mesylate compared with the pure eprosartan mesylate. By solvent immersion/evaporation, the eprosartan mesylate is absorbed by a porous structure. The SEM shows the drug is loaded with crystals and rod-shaped pores. In XRPD, crystallinity of BPSF and unprocessed starch is measured as 26.76 percent and 28.6 percent, respectively. Eprosartan mesylate is thus identified on the surface of BPSF only by FTIR. From the *in vitro* drug release studies, it was confirmed that BPSF can be used to enhance the water solubility of poorly water-soluble drugs. This study demonstrates the great significance of using BPSF as a new delivery mechanism for medicines that are poorly water-soluble based on these results. This method can be used as a replacement for another currently used technique to enhance the stability of poorly soluble drugs.

**Keywords:** Biodegradable Porous Starch Foam (BPSF), Poor water solubility, Eprosartan Mesylate, Bioavailability.

### 1. INTRODUCTION

As a degradable porous biocompatible material based on starch, Biodegradable Porous Starch Foam has huge potential for poorly water-soluble oral dosage forms that have not been investigated to date as a solid dispersion vehicle. Compared to inorganic carriers, Biodegradable Porous Starch Foam has shown strong properties and has a nano-porous structure, low density and large specific surface area and pore volume of Biodegradable Porous Starch Foam to improve the solubility and enhance absorption of poorly water-soluble drugs. These are especially desirable properties for vehicle design for systems of oral drug delivery that are poorly water-soluble [1]. Starch-based polymers have been widely researched for many applications as drug delivery systems, ranging from scaffolds for tissue engineering to bone cement, microparticle drug delivery systems, and hydrogels [2]. The most reliable distribution factor is Starch. General starch foam is formulated using extrusion or microwave strategy by swelling. Perhaps the product of swelling using extrusion or microwave methodologies

is a large pore size of around 1  $\mu$ m [3]. A new method is used for the preparation of Biodegradable Porous Starch via gelatinization associated with the solvent exchange approach. The products obtained have many advantages using this technique, such as a smaller pore size of about 200 nm, generally high throughput, high batch to batch repeatability, and simple scaling. Researchers have also produced countless foam products successfully in the last century, including microcellular starch foams (SMCFs) for volatile compound encapsulation and porous injection-molded starch-based blends for tissue engineering scaffolds. However, the use of Biodegradable Porous Starch Foam as an additive to enhance the aqueous solubility of poorly water-soluble drugs still hasn't been studied in detail.

Eprosartan has indeed been approved for the treatment of hypertensive patients in even more than 20 countries as a non-peptide angiotensin II receptor antagonist (e.g., USA, UK, Germany). The drug is orally active and has a chemical structure that is different from biphenyl and tetrazole [4]. In healthy volunteers, patients with

hypertension, and special patient populations, pharmacokinetic studies of eprosartan have been performed. Plasma concentrations of Eprosartan peak 1 to 3 hours after a fasting oral dose [5]. Changes in  $C_{max}$  and AUC values that do not appear clinically significant were variable (<25%) due to food delay and cause of absorption of eprosartan. Eprosartan plasma concentrations increase proportionally slightly lower than the dose over the 100 mg to 800 mg dose range. The mean terminal elimination half-life of eprosartan was approximately 20 hours after multiple 600 mg oral doses. The absolute drug release was anticipated to be only about 13 percent in a research of 17 human volunteers who received the commercially available oral tablet and the intravenous eprosartan tract formulation. Due to the physico-chemical properties of the drug, the low plasma concentrations of eprosartan may be the product of incomplete absorption [6]. Eprosartan exhibits solubility and hydrophobicity in water dependent on pH, which can result to variable absorption as the compound passes through the gastrointestinal tract. Because the mean and variable absolute bioavailability of Eprosartan is only 13%, effective treatment of hypertension, congestive heart failure and renal failure may necessitate doses of up to 800 mg per day. Also, its mesylate salt is the commercial form of the drug, it can be difficult to swallow high-dose tablets (for example, 600 mg tablets weigh 1000 mg). Eprosartan's bioavailability is limited by solubility, rather than liver metabolism within cytochrome P450. A formulation that improves the bioavailability of eprosartan is therefore required. 4-({2-butyl-5-[2-carboxy-2-(thiophen-2-ylmethyl)-et-1-en-1-yl]-1H-imidazol-1-yl-mono-methanesulphonate} methyl) benzoic acid is eprosartan mesylate. It is a fine white powder which also has poor water solubility. By using BPSF as a carrier system, the present study is an attempt to overcome the poor aqueous solubility of Eprosartan [7].

## 2. MATERIAL AND METHODS

### 2.1. Phase Solubility Study

The solubility phase study was conducted according to the method reported by M. Cirri et.al [8]. Drug and carrier according to the specified drug; the carrier ratio has been precisely weighed and 25 ml of water in screw cap bottles has been added to the neat drug. All of the bottles were shaken at 37°C and 24°C for 24 h on a Remi orbital incubator shaker. The drug-and-water container was used as a control. Solutions were filtered to filter

paper (0.4 nm) after 24 h and the filtrate was diluted. Spectra absorbances were measured at 232 nm. The solubility of the drug was calculated from the absorbance [9].

### 2.2. Preparation of BPSF

A known quantity of 8.0 percent soluble starch and water suspension was heated in a reaction vessel at 100°C for 0.5 h with stirring. The melt has been lowered to 85°C and then poured into a petri dish. In order to promote the gelling, the resulting suspension was cooled in a refrigerator (50°C) overnight. To retain the porous structure of the gel, the gel was then transferred to five volumes of 40 percent, 60 percent, 90 percent, and 100 percent ethanol/water solution, respectively, and modified for 24 hours, so that the ethanol replaced the water in the aqua gel for the Alcolgel to form. By rotary evaporative drying at 300°C, the resulting foam was obtained. Inside the mortar, the dried BPSF was then ground and passed through an 80-mesh display, and the BPSF particles were deposited in a vacuum dryer [1].

### 2.3. Drug Loading in BPSF

BPSF was dried by rotary evaporation heating at 30°C under vacuum for 0.5 h just before Eprosartan Mesylate was embedded. The Eprosartan Mesylate/ethanol solution (20 mg/ml) and the 1/5, 1/10, 1/15 BPSF ratios were combined and stirred at room temperature for 5 hours [1]. The solid powder was dried in the vacuum dryer for 24 h after vacuum-drying. Since adsorption increased with an increased concentration, ethanol was chosen as the dissolution medium and Eprosartan Mesylate has high ethanol solubility [14].

### 2.4. Preparation of the physical mixture

Physical blends of Eprosartan Mesylate/BPSF at a 1:5 proportion were obtained by mixing the individual components in a mortar until the mixture was homogeneous [8].

### 2.5. Characterization of BPSF

#### 2.5.1. Scanning Electron Micrograph Characterization

Using a field emission scanning electron microscope capable of working at an accelerating voltage of 1 kV and a secondary analyzer, the morphology and microstructure of BPSF and loaded BPSF samples were evaluated.

### 2.5.2. *Differential Scanning Colorimetry Characterization*

With a DSC-60 differential scanning calorimeter, Differential Scanning Colorimetry standards were obtained. Readings from 30 to 300°C were obtained at a flow rate of 40 ml/min at a scan rate of 10°C/min under a nitrogen stream.

### 2.5.3. *XRPD Characterization*

XRPD was performed at 30 kV and 30mA Philips using a Cu-K $\alpha$  radiation diffractometer ( $= 1.54\text{\AA}$ ). A Li-F crystal has been used to obtain the monochromatic diffraction beam. In an angular range of 5° (2) to 60°, the powder samples were scanned with a scanning speed of 0.50/ min and a phase size of 0.020.

### 2.5.4. *FTIR Characterization*

Using the KBr pellet technique, Fourier transform Infrared spectra were obtained using an FTIR spectrophotometer. It evaluated the spectroscopic range from 400 to 4000cm<sup>-1</sup>. Each spectrum was collected at a resolution of 2 cm<sup>-1</sup> to obtain a good signal-to-noise ratio (S/N) and high reproducibility, and at an average of 100 repeated scans have been obtained for each run. The observations were all carried out in a dry environment.

### 2.5.5. *In vitro drug release studies*

By measuring the combined dissolution percentage of the BPSF and pure drug released, drug release was calculated using the USP type-II dissolution apparatus, method II (paddle) in 900 ml of phosphate buffer pH 7.0 with Sodium Dodecyl Sulphate at 0.2 percent as a dissolution medium at a temperature of 37±0.5°C. The drug sum was selected such that the final concentration was equivalent to 10 percent of the overall solubility of this drug in 0.2 percent SDSS (immersion conditions). The medium was agitated at 50 rpm and samples were taken at specified times (5, 10, 15, 20, 30, 45 minutes) and the content of eprosartan mesylate at 238 nm was determined by ultraviolet spectrophotometry. By an average of 3 determinations, the amount of drug released from the sample was not explicitly computed. A proportion of the dissolved drug was plotted as the amount of release of the drug versus time [1].

## 3. RESULTS AND DISCUSSION

### 3.1. *Preparation of BPSF*

We have used the solvent exchange technique to prepare BPSF in this analysis. In order to keep the porous

structure of the gel, the exchange solvent is a crucial factor in the displacement of the water from the hydrogel. We selected alcohol to avoid shrinkage and collapse of the aquagel as the exchange solvent, resulting from direct air drying. Alcohol has a lower surface tension than water because it does not solubilize starch and can volatilize easily as opposed to other non-aqueous solvents. The form of starch and the aqueous starch solution's heating temperature and concentration are also closely related to the properties of the BPSF. By solvent immersion/evaporation, the eprosartan mesylate is absorbed by a porous structure. Many pore-scale mechanisms include the processes of drug adsorption due to solvent evaporation, including mass transfer through advection and absorption in the gas phase, viscous flow in the liquid and gas phases, and capillary effects in the pores of the throat-liquid meniscus.

### 3.2. *The morphological and structural characterization of Biodegradable Porous Starch Foam*

In SEM, the morpho structural features of BPSF have been further studied. As in fig. 1, SEM images clearly state that from all nanoscale porous structure samples, BPSF is obtained (approx. 200 nm). A substantial benefit is the cross-connection between pores. Second, it is possible to increase the specific area of the surface; maintain the nanometer range of the size of the drug molecules; prevent congestion and accumulation of the drug particles; retain particle dispersion; decrease the crystal structure of the drug; and improve its stability. Second, from various places, the substance is absorbed through the pores and this simultaneously decreases the resistance to the drug's dispersion into the porous channels. Both of these features foster the drug's dissolution.

### 3.3. *Physicochemical characterization of the loaded Biodegradable Porous Starch Foam samples*

The attachment of a drug to the transporter depends not only on the properties of the drug itself, but also on the physical characteristics of the transporter. Eprosartan mesylate incorporated into BPSF explains SEM, XRPD, DSC, and IR mainly by solvent immersion/evaporation.

#### 3.3.1. *SEM Characterization*

A BPSF particle's surface morphology after grinding was not lost as seen in fig. 2C and 2D. In the form of normal

particles in the generating rod, the crystalline crude drug 2E (eprosartan mesylate). As shown in fig. 2F, is spread by a physical mixture of crude drugs and BPSF. The loaded sample, however, does not exist; the drug is

loaded with crystals and rod-shaped pores, as shown in fig. 2H and 2G. This shows that some eprosartan mesylate, some in BPSF pores, is indicative of the presence of BPSF on its surface.

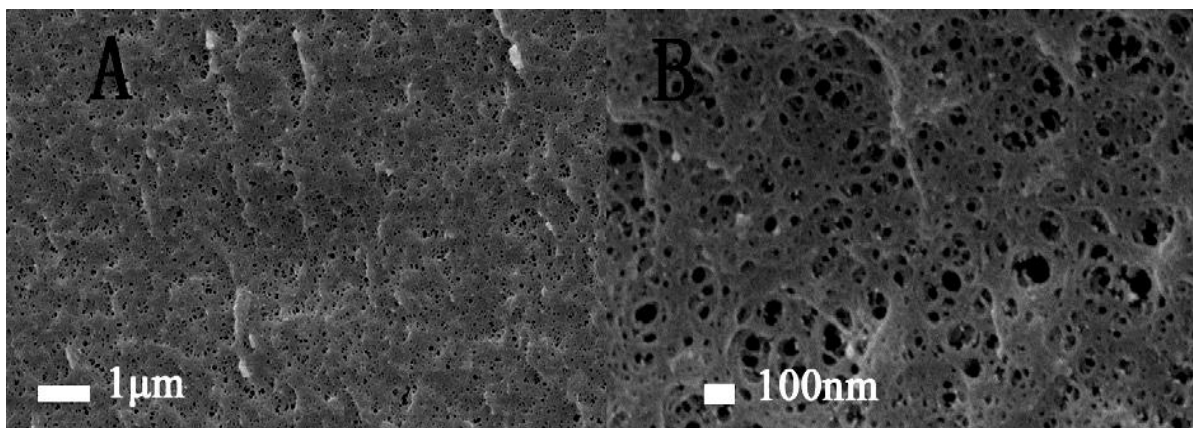


**Fig. 1: The surface feature of cross-section of the BPSF (A and B)**

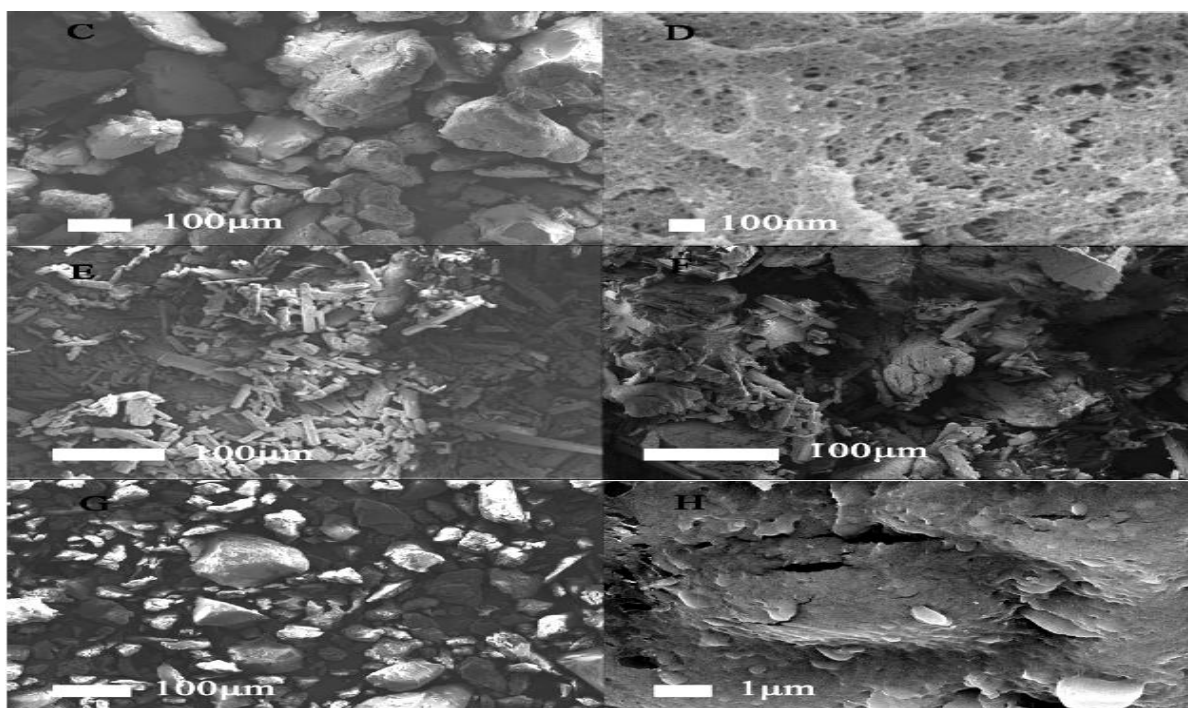


**Fig. 2: The SEM images of BPSF particle after milling (C) and (D), crude drug (E), physical mixture (F), and the loaded BPSF particles (G) and (H)**

### 3.3.2. XRPD Characterization

In fig. 3, the BPSF XRPD standards and the completed BPSF samples can be seen. The BPSF normal, pure eprosartan mesylate, and the physical mixture between eprosartan mesylate and BPSF are added for comparison. The sharp peaks are in the same position as unprocessed starch for pure BPSF. The crystallinity of

BPSF and unprocessed starch is measured as 26.76 percent and 28.6 percent respectively using origin 8.0 software. This means that, as opposed to unprocessed starch, the hardness of BPSF does not really improve. Samples were loaded from sample XRPD standards as in fig. 3, at the same ratio as that of the physical mixture, the loaded sample (1/5 eprosartan mesylate/BPSF) has

a markedly lower pressure, indicating that BPSF adsorption reduces eprosartan mesylate crystallisation. By increasing the amount of BPSF, the XRPD eprosartan mesylate patterns are reduced in the loaded specimens. In comparison, the decrease in particle sizes is evident from the representative peak at  $2\theta = 9.40$  according to the Scherrer formula. The physical mix of 1:5 eprosartan mesylate/BPSF, 1:10 eprosartan mesylate/BPSF, 1:15 eprosartan mesylate/BPSF, 1:5 eprosartan mesylate/BPSF, unprocessed eprosartan mesylate was 19.739 nm, 14.993 nm, 11.314 nm, 29.644 nm, and 38.325 nm. Compared with crude eprosartan mesylate, the particle size of BPSF loaded eprosartan mesylate is smaller. These findings indicate that the particles' large specific surface area increases considerably, which is the primary explanation for improved dissolution. Due to the broad pore diameter of the BPSF spectrum from micropores to mesopores and large pores, eprosartan mesylate absorbed into pores or edges is also found to be partially present as microcrystals, partly amorphously distributed. It still appears that on the surface of BPSF, Eprosartan mesylate exists in crystal form.

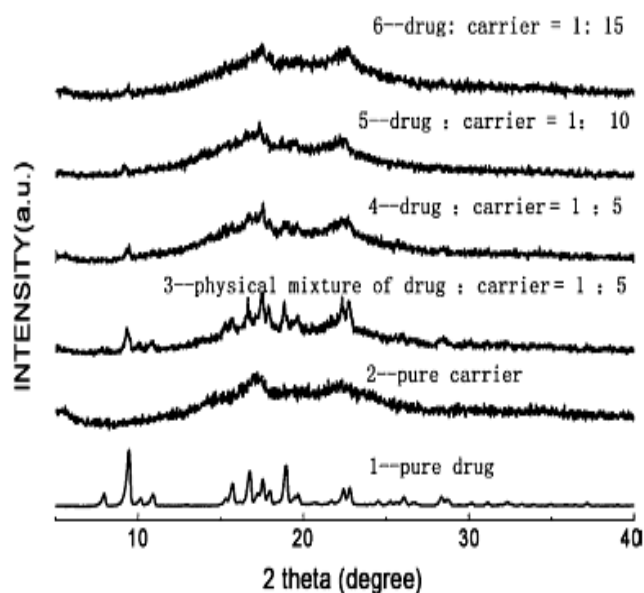


**Fig. 3: The XRPD powder patterns of BPSF, pure Eprosartan Mesylate, its physical mixtures and the loaded BPSF samples**

### 3.3.3. Differential scanning calorimetry (DSC) Characterization

The crude eprosartan mesylate has a melting point of  $175.350^{\circ}\text{C}$ . In relation to the loaded samples, their

respective physical mixture of BPSF and tidy BPSF is seen. Indeed, the loaded sample has a wider and lower freezing peak (eprosartan mesylate/BPSF 1: 5) than the physical mixture with the same ratio, and there is also a wider and lower eprosartan mesylate freezing peak with an increased BPSF ratio. The initial physical mix (eprosartan mesylate/BPSF 1:5) and pure drug temperatures are  $170.26^{\circ}\text{C}$  and  $170.80^{\circ}\text{C}$ , while the respective loaded specimens are  $166.27^{\circ}\text{C}$ ,  $165.07^{\circ}\text{C}$  and  $162.25^{\circ}\text{C}$ , corresponding to 1:5 eprosartan mesylate /BPSF, 1:10 eprosartan mesylate/BPSF, 1:15 eprosartan mesylate/BPSF, respectively, by an improved BPSF ratio. The peak temperature for the loaded samples is about  $50^{\circ}\text{C}$ , lower than for the pure drug ( $170.450^{\circ}\text{C}$ ) ( $175.350^{\circ}\text{C}$ ) as shown in Fig. 4.

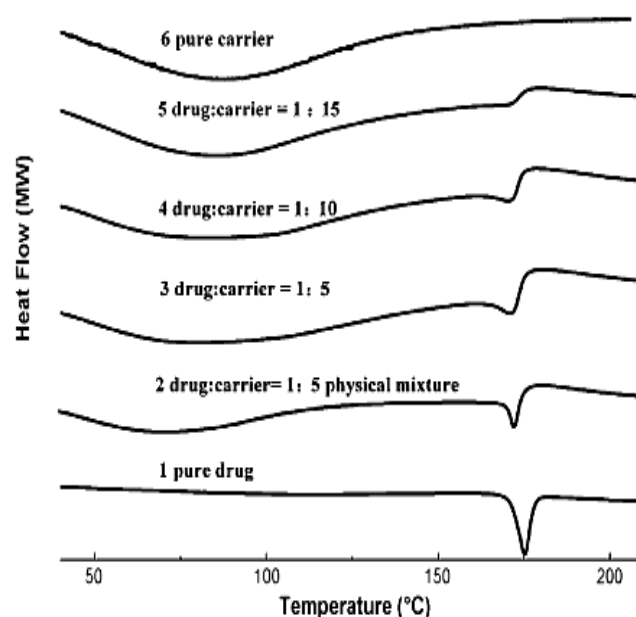


**Fig. 4: DSC patterns of BPSF, pure Eprosartan Mesylate, its physical mixtures and the loaded BPSF samples**

### 3.3.4. Fourier-Transform Infrared Spectroscopy Characterization

The infrared spectra obtained for BPSF, the raw mesylate of eprosartan, the physical mixture and the samples loaded are shown in fig. 5. No new peaks with the usual properties of the loaded samples are seen compared to the physical mixture of BPSF and crude eprosartan mesylate. Proving that there might be no BPSF-eprosartan mesylate interaction or peak position migration characteristic. These results show that the absorption into BPSF of eprosartan mesylate is physical.

With respect to  $3000\text{-}3500\text{cm}^{-1}$  (-OH stretch), BPSF's FTIR spectra have peaks, indicating that BPSF also has a stable structure with several hydrophilic hydroxyl groups. In the loaded sample (eprosartan mesylate/BPSF 1:5), the carbonyl peak of the  $1725.8\text{ cm}^{-1}$  eprosartan mesylate is weaker than that of the physical mixture with the same ratio, and with an increase in the amount of BPSF, the eprosartan mesylate melting peak is also lower. Even though BPSF has a very large specific area for light dispersion (air-solid interfaces), fine particles of BPSF are very effective in dispersing light and have high opacity ability. Eprosartan mesylate is thus identified on the surface of BPSF only by FTIR. The loaded sample (eprosartan mesylate/BPSF 1:5) has significantly lower carbonyl peak intensity than the same-ratio physical mixture, indicating that eprosartan mesylate has been loaded with the BPSF pores. However, most of the eprosartan mesylate remains on the surface of the BPSF.

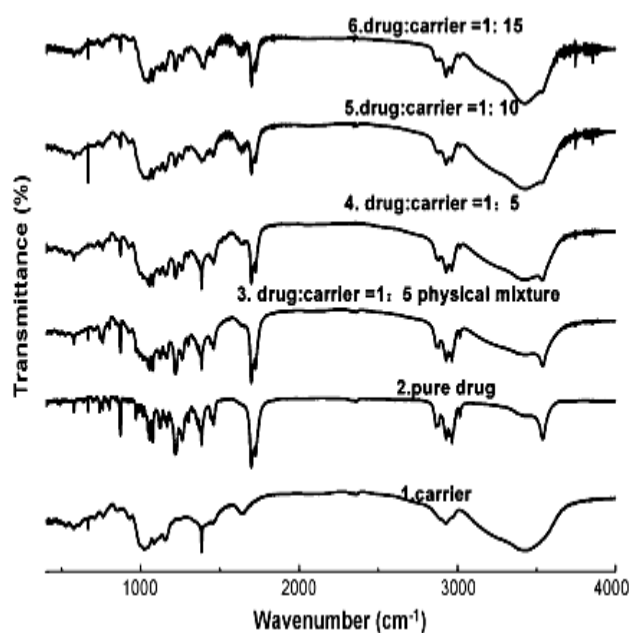


**Fig. 5: The FTIR spectra obtained for BPSF, pure Eprosartan Mesylate, physical mixture and the loaded BPSF samples**

### 3.3.5. *In vitro* drug release studies of the loaded Biodegradable Porous Starch Foam samples

These were found to generate rapid diffusion of eprosartan mesylate as a vehicle for the poorly soluble water-soluble drug using hydrophilic BPSF. As already mentioned in fig. 6, BPSF-loaded eprosartan mesylate has a rapid drug release rate of 80 percent in 15

minutes, as opposed to the existing commercial entity's 45 minutes for the same ratio. Approximately 50 percent of eprosartan mesylate is released in the first 5 minutes, demonstrating a major burst-release effect, while the rest follows a normal extended release pattern and dissolves quickly and evenly over a 40-minute span. Eprosartan mesylate, loaded on internal channels and BPSF surfaces, demonstrates a different release pattern.

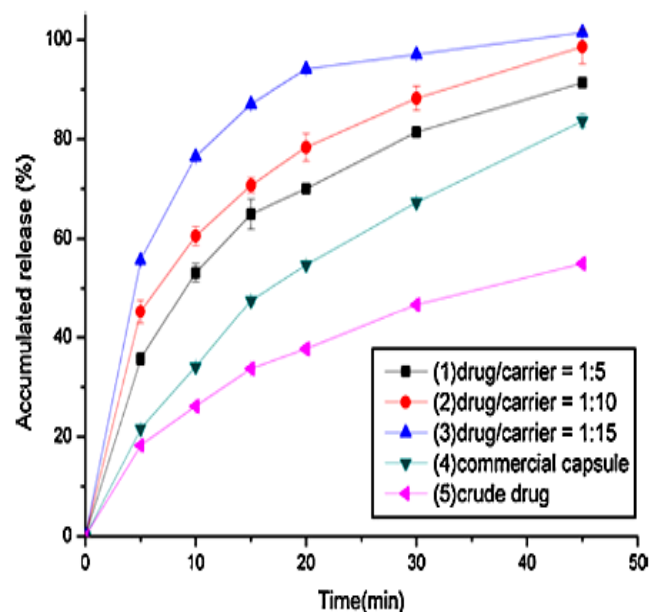


**Fig. 6: *In vitro* drug cumulative dissolution percentage patterns of the loaded BPSF samples, crude drug and commercial capsule**

## 4. CONCLUSION

A low-density, high specific surface area, honeycomb shape and high pore volume biodegradable porous starch foam (BPSF) were obtained for oral bioavailability of poorly water-soluble drugs and their structure was determined by SEM, XRD, DSC, and FTIR that eprosartan mesylate absorbed in BPSF was partially present as microcrystals and partially distributed in the amorphous state in BPSF pores. *In vitro* drug release studies indicated that accelerated immediate release of eprosartan mesylate was developed by the BPSF carrier and improved its oral bioavailability compared with crude eprosartan mesylate and commercial capsules. This study demonstrates the great significance of using BPSF as a new delivery mechanism for medicines that are poorly water-soluble based on these results. This method can be used as a replacement for another currently used technique to enhance the stability of poorly soluble drugs.

## 5. ACKNOWLEDGEMENTS

The authors are grateful to Modern college of Pharmacy, Nigdi, Pune for providing laboratory support.

### Conflict of interest

The authors report no conflict of interest.

## 6. REFERENCES

1. Wu Chao, Zhongyan Wang, Zhuangzhi Zhi, Tongying Jiang, Jinghai Zhang, Siling Wang. *International journal of pharmaceuticals*, 2011; **1(2)**:162-169.
2. Cannava C, Crupi V, Ficarra P, Guardo M, Majolino D, Stancanelli R, et al. *Vibrational Spectroscopy*, 2008; **48(2)**:172-178.
3. Bella G R, RS Jeba Jeevitha, S Avila Thanga Booshan. *Int J Curr Res Chem Pharm Sci*, 2016; **3**:43-50.
4. Rewar S, Singh CJ. *Int. J. Curr. Res. Chem. Pharma*, 2014; **1(10)**:101-114.
5. Ahn Jae-Soon, Kang-Min Kim, Chan-Young Ko, Jae-Seon Kang. *Bulletin of the Korean Chemical Society*, 2011; **32(5)**:1587-1592.
6. Torres Fernando G, Aldo R Boccaccini, Omar P Troncoso. *Journal of applied polymer science*, 2007; **103(2)**:1332-1339.
7. Bureiko A, Anna T, Nina K, Victor S. *Advances in colloid and interface science*, 2015; **222**:670-677.
8. Cirri M, Mura P, Rabasco AM, Gines JM, Moyano JR. *Drug development and industrial pharmacy*, 2004; **30(1)**:65-74.
9. Wang Miao, Sung-Kyun You, Hong-Ki Lee, Min-Gu Han, Hyeon-Min Lee, Thi Mai Anh Pham, et al. *Pharmaceutics*, 2020; **12(6)**:544.
10. Pham TTH, Loiseau PM, Barratt G. *International journal of pharmaceuticals*. 2013; **454(1)**:539-552.
11. Soykeabkaew N, Chuleeporn T, Orawan S. *Composites Part A: Applied Science and Manufacturing*, 2015; **78**:246-263.
12. Jiang T, Chao Wu, Yikun G, Wenquan Zhu, Long Wan, Zhanyou Wang, et al. *Drug development and industrial pharmacy*, 2014; **40(2)**:252-259.
13. Jin, Zhengyu. *Functional starch and applications in food*. Springer. 2018.
14. Hou Yu, Yan Xia, Yongkang Pan, Songchao Tang, Xiaofei Sun, Yang Xie, et al. *Materials Science and Engineering*, 2017; **76**:340-349.
15. Wu Chao, Jing Wang, Yanchen Hu, Zhuangzhi Zhi, Tongying Jiang, Jinghai Zhang, et al. *Materials Science and Engineering*. 2012; **32(2)**:201-206.
16. Achulatlal H, Rao VU, Sudhakar M. *Open J Adv Drug Deliv*, 2014; **2(4)**:576-584.
17. Ghorbani M, Leila R. *International Journal of Polymeric Materials and Polymeric Biomaterials*, 2021; **70(2)**:142-148.
18. Bureiko A, Anna T, Nina K, Victor S. *Advances in colloid and interface science*, 2015; **222**:670-677.